# Chapter 1

# Introduction

## 1.1 Ultraviolet & X-ray Radiation in Astrophysics

Light of shorter wavelengths than our optical spectrum ($\lambda \lesssim 320$ nm) is regarded here as *high energy* radiation. This is because it is light that is too energetic for the receptors in our eyes to process - just beyond the colour violet, the *ultra*violet is the wavelength range between 10 nm $\lesssim \lambda \lesssim$ 320 nm (*ultra* means 'beyond' in Latin). At even smaller and more energetic wavelengths is the *X-ray* regime between 0.1 nm $\lesssim \lambda \lesssim$ 10 nm. Like any part of the electromagnetic spectrum, UV and X-ray photons are emitted by astrophysical particles accelerating from forces, and all four fundamental forces are responsible for high energy astrophysical radiation. The majority of processes discussed in the context of Galactic X-ray sources originate from electromagnetic and gravitational forces.

In general, *Larmor's Formula* describes the power emitted by a particle of charge $q$ undergoing acceleration $a$ (non-relativistic, $v << c$):

$$P = \frac{q^2 a^2}{6\pi\epsilon_0 c^3} \quad \text{(Watts)} \tag{1.1}$$

where $c \simeq 3 \times 10^8$ m/s (the speed of light) and $\epsilon_0 \simeq 8.854 \times 10^{-12}$ F m$^{-1}$. A careful consideration of the acceleration mechanism for each particle and a sum over all accelerating particles yields the volume emissivity $j_\nu$. X-ray emission mechanisms usually require high energy electrons (large $\beta$, where $\beta = \frac{v}{c}$) and so the special relativistic formulation is useful:

$$P = \frac{2q^2\gamma^6}{3c}[\dot{\beta} - (\beta \times \dot{\beta})^2] \quad \text{(Watts)} \tag{1.2}$$

where $\gamma = (1 - \beta^2)^{-1/2}$.

There are a variety of X-ray emitting objects and associated processes spanning a range of X-ray luminosities $L_X$. Although our focus will be on *Galactic* X-ray emission we mention some extraGalactic X-ray sources here for completeness. X-ray point sources include both degenerate and non-degenerate stars, compact and non-compact binary systems, active Galactic nuclei (AGN) and star forming regions (e.g., Orion Nebula or h Per). Diffuse X-ray sources include supernovae remnants (e.g., Crab Nebula, Cassiopeia A), all types of galaxies, galaxy groups and clusters (e.g., Perseus Cluster, M87) and even planets (e.g., Jupiter) and comets (e.g., 73P/Schwassman-Wachmann). The focus of this work is to identify compact binary systems and therefore the bulk of this discussion will be focussed on X-ray point sources.

The most basic production mechanism of high energy light is *thermal emission* from hot, optically thick matter where particles accelerate due to electromagnetic interactions from neighbouring particles. A star is roughly a blackbody emitter due to high temperature and densities (at least below the photosphere) and its light spectrum is governed broadly by *Planck's Law* or 'the blackbody function'

$$B(\lambda, T) = \frac{2hc^2}{\lambda^5} \frac{1}{e^{\frac{hc}{\lambda kT}} - 1} \quad \text{(W sr}^{-1}\text{ m}^{-3}\text{)} \tag{1.3}$$

where $h = 6.63 \times 10^{-34}$ m$^2$ kg s$^{-1}$ (Planck's constant), $k = 1.38 \times 10^{-23}$ m$^2$

kg $s^{-1}$ (Boltzmann's constant) and $T$ the effective temperature of the star in Kelvin. The Planck Distribution describes the spectral density of emitted photons in equilibrium and is the unique, stable such distribution (Planck 1914). It describes hot, dense matter like the thermal emission from a star or a hot, optically thick accretion disk in both CVs and X-ray binaries (XRBs). As temperature increases the peak of emission shifts to higher energies following Wien's Law:

$$\lambda_{peak} = \frac{b}{T} \quad \text{(m)} \tag{1.4}$$

where $b = 2.898 \times 10^{-3}$ m K. Stars peaking at the least energetic part of the UV spectrum ($\sim$ 320 nm) need to achieve effective temperatures of $T \simeq 9000$K or an earlier spectral type than $\sim$A3V. To peak in the X-ray (say at 1nm) the temperature needs to reach $T \sim 3 \times 10^6$ K. These (effective) temperatures cannot be reached by non-compact stars in regular stellar evolution but are easily achieved in material liberating its energy in the steep gravitational potential of a CO. Thermal emission from a single non-degenerate star is usually insufficient to explain observed X-ray luminosities $L_X > 10^{29}$ erg/s and it is non-blackbody processes responsible for X-ray emission in regular stars. Optically thin radiation from hot, ionized material is common in binary accretion scenarios and stellar atmospheres. The principal non-relativistic radiation mechanism from hot, ionized material is *thermal bremsstrahlung* or 'braking radiation', where high speed electrons accelerate around more massive protons in the plasma. The volume emissivity of thermal bremsstrahlung emission as a function of temperature is:

$$j_\nu(\nu) = C g(\nu, T, Z) Z^2 n_e n_i \frac{e^{-\frac{h\nu}{kT}}}{T^{\frac{1}{2}}} \quad \text{(W m}^{-3}\text{ Hz}^{-1}\text{)} \tag{1.5}$$

where $C = 6.8 \times 10^{-51}$ J m $K^{\frac{1}{2}}$, $g(\nu, T, Z)$ is the Gaunt factor (a quantum correction of order $\sim$ 1), $Z$ is the atomic number of the atomic species, $n$ is density, and $T$ temperature. For temperatures between $10^5 - 10^8$ K this

distribution peaks in the extreme ultraviolet (EUV) or soft X-ray.

### 1.1.1 Single Stars

Thermal emission from both optically thick and thin bodies explains a large portion of the spectral energy distribution of single stars. The stellar temperature profile $T(r)$ is generally a decreasing function of radius but inverts in the outermost region or *corona* of many cool stars (including the Sun); we observe spectral features only produced in temperatures of $10^6$-$10^7$ K (for example, transitions of the ionic species Fe-XIV at 5303 Å and Fe-X at 6374 Å in the Sun) prompting an explanation of some unknown coronal energy source. Temperature inversion and emission in excess of radiative equilibrium is more or less the definition of the corona itself (Hall, 2008).

The behaviour of hot, magnetically-confined coronal plasma is known as *chromospheric* or *coronal* activity observed as emission in excess of the blackbody at short wavelengths (UV, X-ray, $\gamma$-Ray). All late-type stars (past $\sim A7$) are coronal X-ray emitters (Vaiana et al., 1981). Stellar coronae are physically extended, optically thin plasmas that are a source of both line and continuum UV/X-ray. They are highly ionized by the photospheric flux below and emit at $T \sim 10^7$K soft-X-ray continuum via *thermal bremsstrahlung* (Section 1.1). The layer beneath the corona (the chromosphere) produces Ca II H & K emission lines in abundance and these lines are generally used as indicators of coronal activity levels (West et al., 2008).

The interaction of the coronal plasma and the stellar magnetic field is likely the source of coronal heating. Velocity shear from differential rotation between the convection cells and the radiative zone energetically drive large-scale, variable magnetic structures which thread high through the corona (the *dynamo* mechanism). These fields interact strongly with the plasma by induction, and production of magnetohydrodynamical (MHD) waves that heat the surroundings (Hall, 2008). The plasma and the magnetic field lines are both mag-

netic - the movement of either component induces complex changes in both. The short-timescale variability of the corona (seconds to minutes) reflects the timescale of changes in the magnetic field structure itself.

Although it is not our intent to study stellar rotators in general, a macro-connection between late-type stars and their induced X-ray luminosities is helpful. The ability for the dynamo to produce magnetic activity or the *dynamo efficiency* is typically characterized by the *Rossby Number* (Noyes et al., 1984) which combines the rotation rate $P_{rot}$ and convective turnover time $\tau_c$ (the rotation rate of the convection cell):

$$R_0 = \frac{P_{rot}}{\tau_c} \tag{1.6}$$

Stellar activity typically increases with decreasing $R_0$ and it is observed that late-type stars saturate in their coronal X-ray emission at $\mathrm{R_0} \simeq 0.1$ (Vilhu, 1984; Stepien, 1994; Patten and Simon, 1996; Pizzolato et al., 2003) where higher rotation rates do not add any extra flux in the X-ray and in fact may *decrease* with a further increase in rotational frequency. The relation between $R_0$, $R_X = L_X/L_{bol}$ and $P_{rot}$ is shown in Figure 1.1 (Wright et al., 2011, Figure 2).

The convective turnover time can be estimated as a function of stellar mass following Wright et al. (2011) as a second-order log-log polynomial,

$$\log(\tau_c) = 1.16 - 1.49\log(M/M_\odot) - 0.54\log^2(M/M_\odot), \tag{1.7}$$

with an rms dispersion in $\log(\tau_c)$-space of $\sim$0.028. This relation is valid for MS masses $0.09 < M/M_\odot < 1.36$ but is highly uncertain for $M < 0.15M_\odot$ due to a lack of data for the lowest-mass stars. Other parameterizations as functions of $V - K_s$ and $B - V$ exist but they are not nearly as tight, and even be piece-wise; convection may be driven primarily by the stellar mass and complex-colour dependencies on various stellar parameters make a $\tau(M/M_\odot)$

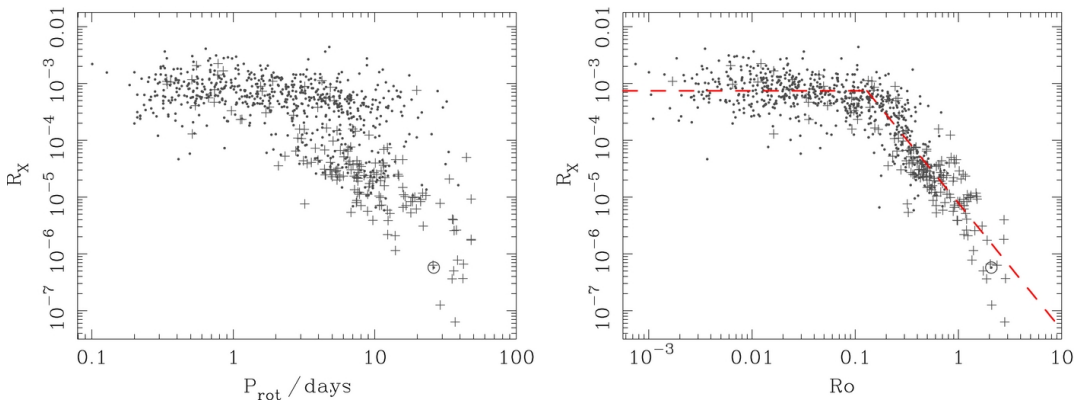


Figure 1.1: (left) $R_X = L_X/L_{bol}$ by rotational period and (right) by the Rossby number. Notice the parameterization with $R_0$ is far tighter than $P_{rot}$, and as expected X-ray luminosity increases with decreased rotational period or $R_0$. The piece-wise, red dashed line represents the unsaturated (sloped) and saturated (flat) regimes (Wright et al., 2011, Figure 2).

parameterization most useful.

Summarily, the rotation period and stellar mass are connected via the Rossby number, which is itself connected to X-ray luminosity. We summarize this discussion by showing X-ray luminosity versus stellar mass (Figure 1.2) using Equations 1.6 and 1.7 together for some values of rotational period $P_0$.

Stellar magnetic fields can undergo explosive, short-timescale changes (*magnetic reconnection*) that produce solar flares and coronal mass ejections that manifest as a burst of hard X-ray emission, followed by a soft rise from the X-ray heating of the upper atmosphere. Magnetic reconnection occurs when a magnetic field loop pinches in two after being highly stressed. The rapid change in the $B$ field strength over only a few seconds creates an intense DC electric field $E$ that accelerates electrons beyond $\sim$20 keV (Hall, 2008). These electrons stream back into the stellar atmosphere and undergo (inefficient) Coulomb collisions with ambient protons, emitting a burst of hard X-rays - this process is known as *non-thermal bremsstrahlung* or *thick target bremsstrahlung*. A short burst of hard X-rays is almost always observed at the beginning of a flare event and is usually used as an indicator of the event itself. The hard X-rays heat and

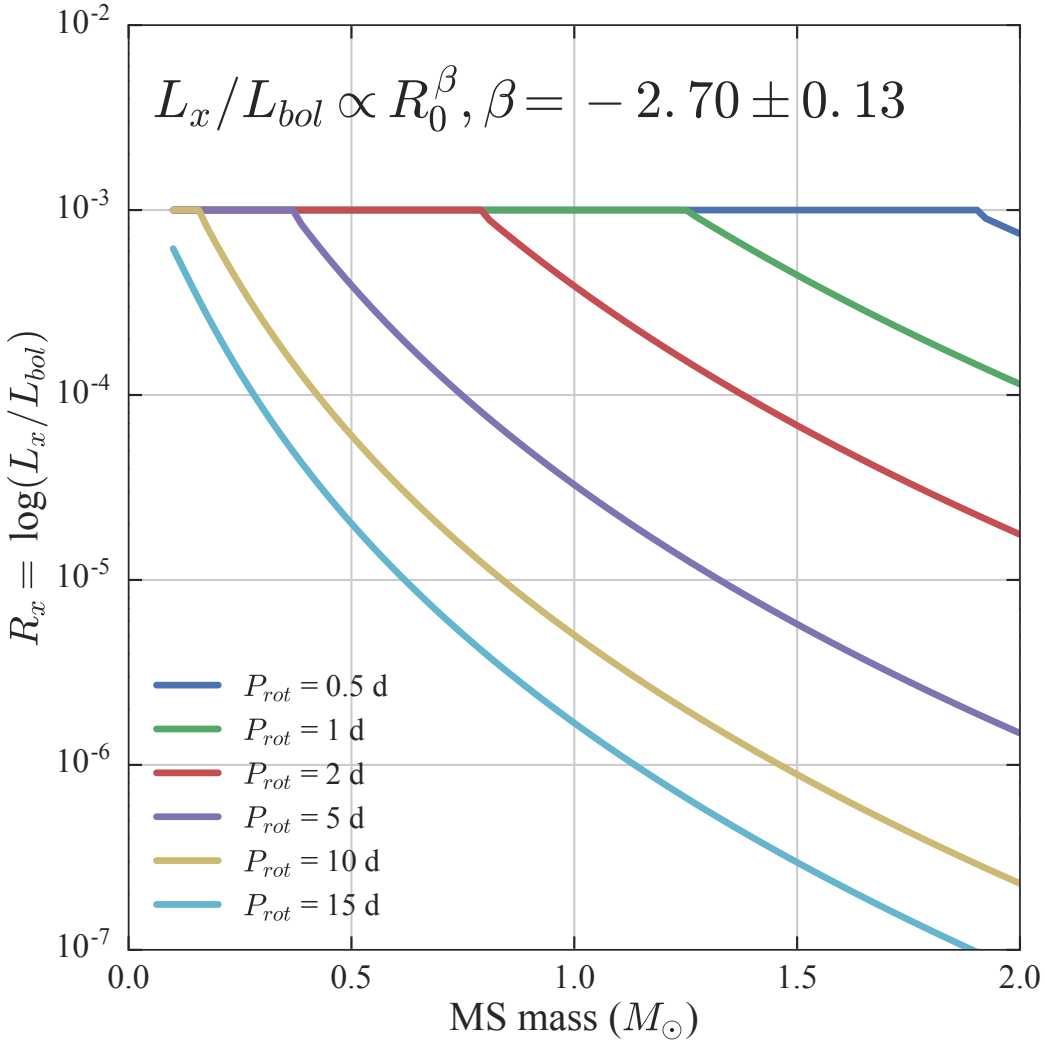


Figure 1.2: $R_X$ as a function of stellar-mass for a few values of rotational period $P_{rot}$. Saturation occurs at $R_X = 10^{-3}$. Only $M_\odot > 0.1$ are shown, for the relationship is uncertain beyond this range (Wright et al., 2011). It appears that no stellar mass can saturate at a rotational period above $\sim 10 - 15$d.

create a pressure gradient driving bulk plasma motion that emits soft X-rays in the process. This bulk flow is likely responsible for the time delay between the rise in hard versus soft X-rays immediately after a flare (Güdel, 2004). Non-thermal bremsstrahlung is thought to be the main contributor of hard X-rays in single-stellar atmospheres and their presence is often more sporadic (burst-like) than the soft coronal continuum.

In summary, single-stars are X-ray/UV emitters up to $L_X \sim 10^{30}$ erg/s due to their hot, coronal plasma interacting with the stellar magnetic field.

### 1.1.2 Compact Binary Systems

#### Formation of a Compact Object

All stars undergo *stellar evolution* where the temperature, composition, and radius of the star change over their lifetime. The outcome of stellar evolution in isolation is almost entirely determined by the initial mass of the star. In general, a star maintains a quasi-equilibrium between the inward pull of gravity and outward thermal pressure that originates from formation energy and ongoing nuclear fusion in the core.

A star spends the majority of its lifetime on the main-sequence (MS) fusing core H into He until H runs out and the burning equilibrium is disrupted. Without the core pressure from H fusion, the core begins to contract and H fusion is initiated in a shell around the predominantly He core, stabilizing the contraction. This shell burns hotter than the core-burning itself and increases the luminosity of the star leading to an envelope expansion. As each burning layer runs out of fuel, the resultant fusion products add to the core mass, shrinking it further, igniting the new shell layers and expanding the star while ascending the red giant branch (RGB). From here, the star moves through the horizontal branch (HB) and asymptotic giant branch (AGB), where large mass-loss can occur from stellar winds before the end of its life. What happens

next is strongly dependent on the core mass ($\sim$ original mass - mass lost during lifetime): for stars with $M < 8M_{\odot}$ thermal pressure eventually becomes insufficient to balance gravity and the star contracts until it is supported by degenerate electron pressure, resulting from both Heisenberg's uncertainty and Pauli exclusion principles. Heisenberg's Uncertainty Principle states that the ignorance of a particle's momentum and position in space has a lower limit of roughly $\hbar$:

$$\Delta x \Delta p \geq \frac{\hbar}{2} \tag{1.8}$$

The core of a star with an initial mass $M < 8M_{\odot}$ can be supported by *electron degeneracy pressure*. Such a core is referred to as a *white dwarf* (WD). The Pauli exclusion principle forbids the electrons from occupying the same phase space cell manifesting as a resistive pressure. WDs are $\sim$ the size of earth and typically $\sim 0.6M_{\odot}$ with densities of $\rho \sim 10^9$ kg/m$^3$; binaries with a WD primary accreting from a companion are known as *cataclysmic variables* (CVs; see Section 1.1.2).

Electron degeneracy pressure cannot support the cores of stars of initial mass $M > 8M_{\odot}$ against collapse and instead *neutron* degeneracy pressure exists, leaving a *neutron star*. It is thought to be the size of a small city ($R \sim 10 - 15$ km) with average densities exceeding $\sim 10^{17}$ kg/m$^3$. Neutrons are $\sim 2000$ times heavier than electrons and thus their momentum uncertainties $\Delta p$ can be quite large. Thus, $\Delta x$ can be much smaller than the electron allowing neutrons to spatially pack themselves more closely (neutron stars are $\sim$ a factor of a billion more dense on average than WDs). If the stellar core mass is high enough ($M > 20M_{\odot}$) there exists no degenerate pressure strong enough to counter the gravitational collapse, and the star becomes a black hole.

### Accretion in Compact Binaries

The deep gravitational wells of a CO can inject hugh energies into nearby material, including other stars. Binaries with one or more components consisting of a WD, NS or BH in a close orbit ($a \sim$ order of the donor's radius) are referred to here as *compact binary systems*. They can emit a copious amount of X-rays ($10^{30} \sim 10^{42}$ erg/s) and show distinct states of activity that dramatically change the emission behaviour. The movement of material from the companion star to the compact primary is known as *accretion*, and this process is responsible for the macroscopic behaviour of compact binaries. Different stages of accretion and the response of the mass ratio $q$ and orbital separation $a$ to these modes ultimately decides the long-term evolution of the binary.

There are two types of accreting binaries: *transient* systems that go in and out of outburst and *persistent* systems that are in constant outburst. The mass ratio $q = M_{CO}/M_{donor}$ and donor radial velocity $K_2$ are two fundamental binary parameters that describe the accretion. It is not our intent to review accretion theory entirely, a basic understanding of these parameters is helpful. The parameters $q$ and $K_2$ are usually obtained in quiescence with optical or IR spectroscopy when the dimness of the accretion disk allows study of the companion. Combining $K_2$ and $P_{orb}$ directly limits the value of $q$, where this relation is detailed by the *mass function* (derived from Kepler's 3rd Law):

$$f(M_1) = \frac{PK_2^3}{2\pi G} = \frac{M_1 \sin^3(i)}{(1+q)^2} \tag{1.9}$$

where $i$ is the inclination (the angle between a line perpendicular to the system orbital plane and our line of sight, e.g., an edge-on system has inclination 90°); this parameter is often difficult to obtain. If the system in quiescence still has a large optical contribution from the disk, $K_2$ can be derived from its linear relation with the full-width-half-maximum (FWHM) of the $H\alpha$ line in the accretion disk (Casares, 2015, 2016). Persistent sources are constantly in

outburst and therefore bright in the optical, UV and X-ray. These bands are dominated by the CO and disk and are never in quiescence which wash out the companion's spectral features. In these cases, the companion's radial velocity can be derived by tracking a series of fluorescent emission lines from the X-ray irradiated companion face during certain parts of the orbit. These emission features from the companion face are known as *Bowen fluorescence transitions* (Casares et al., 2003, 2004; Sánchez et al., 2015).

Finally, the mass ratio $q$ and semi-major axis $a$ define the geometry of the gravitational potential in the system of two stars. It is this geometry that controls the accretion process; local extrema in the potential (*Lagrange points*) represent places where material can remain in a stable co-orbit or where matter can leave one star and be bound to the other. As the companion expands during stellar evolution, it may fill the volume around it known as the *Roche Lobe* which is the smallest surface of equipotential, defined by the scale radius $R_L$:

$$\frac{R_L}{a} \simeq \frac{2}{3^{4/3}}\left(\frac{q}{1+q}\right)^{1/3} \tag{1.10}$$

Material exceeding this volume is no longer bound to the donor; material preferentially leaves through the first Langrangian point (L1) at a distance $\sim R_L$ from the center of the donor. The ability for a star (at a particular part of its life cycle) to fill this lobe and lose mass depends solely on $a$ and the mass ratio, $q$. The Coriolis force deflects the accretion stream into Keplerian motion around the primary, but the stream may couple to the field and accrete directly onto the primary if its magnetic field is strong enough. Small collisions of the streaming particles with each other (e.g., viscous friction) spread the orbital radii of the particles forming an accretion disk truncated at the Alfven radius of the primary. The interactions between the donor, accretion stream/disk, magnetic field(s), stellar winds and compact object create the variety of high energy radiation we attribute with the name "X-ray binary".

Here we review compact systems relevant to this thesis: CVs, symbiotics

and low-mass XRBs with specific focus on the systems appearance in the X-ray, UV and optical components of the spectral energy distribution (SED).

### Cataclysmic Variables

Cataclysmic variables or CVs are close binary systems of a WD primary and a Roche-Lobe-filling donor, with orbital periods 75 min $< P_{orb} <$ 8 h capable of X-ray luminosities of $L_X \simeq 10^{29} - 10^{33}$ erg/s (Ritter and Kolb, 2003). The majority of CV donors are Roche-lobe-filling MS stars but there exist systems with a less massive WD donor (AM CVn) or a giant donor (symbiotic systems). The short and long-term behaviours of CVs depend primarily on the mass transfer rate $\dot{M}$ and magnetic strength $B$ of the WD and their interaction determines the accretion state (Lewin and van der Klis, 2006).

CVs with weak WD magnetic fields ($B \lesssim 10^4$ G) are essentially 'non-magnetic'; accreting material can accumulate in an *accretion disk* that interacts with the WD close to its surface, in a region called the *boundary layer*. This boundary layer is thought to be the primary source of both soft and hard X-rays in CVs. The accretion disk acts as a resevoir of gas and ultimately energy for the outburst behaviour of CVs and XRBs alike. Non-magnetic CVs can be in either quiescence or outburst, controlled by $\dot{M}$: when $\dot{M}$ is low, the disk is cool and has a low viscosity. When the disk heats, its viscosity increases allowing movement of material inward towards the WD inducing direct accretion - this is the high $\dot{M}$ regime. The inward movement of disk material liberates gravitational energy producing a bright, explosive outburst known as a *dwarf nova* (DN). *Nova-like* (NL) systems have a high enough $\dot{M}$ that the disk is maintained in high temperature/viscosity equilibrium and does not exhibit typical DNe (Honeycutt, 2001). The accretion stream, disk and the boundary layer can in principle be seen in a spectral energy distribution (SED) and are inherently variable in the optical, UV and X-ray outside of that expected from orbital geometry changes on timescales $\tau \sim P_{orb}$. In short $P_{orb}$ non-magnetic

CVs, the accretion disk usually contributes 40-75% of the observed optical light while the WD contributes 75-90% of observed UV (Szkody et al., 2017). Systems with disks (DNe or NLs) ostensibly can be identified by their SED given the large fractions of optical/UV light emitted from the WD and surrounding material.

If the WD $B$ field is strong enough ($B > 10^4$ G) it either completely prevents an accretion disk from forming (a *polar* system) or truncates the disk at some distance from the WD (an *intermediate polar* system). In polars, the accretion stream couples to the magnetic field lines between the donor and the WD and is channeled to one or two regions near the WD surface. This produces a noticeable cyclotron spectrum from the IR to the UV (Wickramasinghe and Ferrario, 2000; Williams et al., 2007) from spiraling electrons in the $B$ field and X-rays from shock heating at WD surface (Lewin and van der Klis, 2006). Polars are primarily soft X-ray sources, typically peaking in the EUV where instrument sensitivity is low and interstellar absorption is extremely high. This leaves polars far less studied than non-magnetic CVs. Although polars lack an accretion disk, the accretion stream and shock-spot near the WD surface can be incredibly bright, contributing $\sim$50% of the total optical emission (Harrop-Allin et al., 1999).

In summary, both magnetic and non-magnetic CVs emit X-ray light beyond the active single-stellar emission discussed in Section 1.1.1. The emission of X-rays comes primarily from the WD surface, where direct accretion takes place. However, many components of the system emit relevant radiation: the boundary layer, the disk and/or magnetic field structure, the accretion stream and collision point and the irradiated companion face. In Section 1.1.2 we will explore how similar systems with a neutron star (NS) instead of a WD changes the system's dynamics.

### Symbiotic Stars

Symbiotic binary stars (SBs) are a distinct class of CV where a WD accretes the stellar winds of a red giant donor (Kenyon and Webbink, 1984; Sokoloski, 2003). These systems exhibit various outburst-like behaviours, probably related to Bondi-Hoyle type accretion onto the WD surface but this is not yet fully understood (Sion and Starrfield, 1994). We refer to those with a WD primary as SBs and those with a NS or BH primary as *symbiotic XRBs*. Unlike typical CVs, SB accretion is fed by the giant's wind where only a small portion is actually accreted (owing to the geometrical extent of the wind and the comparatively small cross-section of the WD). SBs show prominent emission features in low resolution spectroscopy (e.g., TiO features from the red giant photosphere and H I, He II and OIII in emission) thought to be emitted from H shell-burning on the WD surface and photoionization of the giant's wind. These emission features have been used historically to identify such systems, however there are SBs that show peculiar outburst behaviours, lack one or more distinct emission features or have a NS or BH primary making the definition of SBs broader than previously thought. Luna et al. (2013) adopt a more general definition of any compact object accreting enough material from a red giant companion to be observed at any wavelength, but we limit this summary to the most abundant WD SBs. In light of this updated definition, the known population of Galactic SBs is probably biased towards shell-burning types which show the aforementioned prominent optical lines in low-resolution spectroscopy (Mukai et al., 2016). Shell-burning SBs burn H steadily on the surface of the WD similar to post-novae behavior or supersoft X-ray emission, and show steady UV emission while *non*-shell burning systems show variable UV emission on short timescales, interpreted as a flickering of the accretion disk (Luna et al., 2013). UV timeseries data in combination with confident counterpart identification in IR surveys like *2MASS* and *WISE* could uncover previously unidentified SBs given recent advancements in near and mid IR

classifications of SBs (Akras et al., 2017).

### Low Mass X-ray Binaries (LMXBs)

Low-mass XRBs (LMXBs) consist of a NS or BH primary with a low mass ($M \leqslant 1M_{\odot}$), Roche-Lobe-filling donor with short orbital periods ($<$ 6h) and X-ray luminosities between $10^{32} < L_X < 10^{39}$ erg/s. These are observed as steady X-ray systems; X-ray studies typically determine the primary properties and optical/IR studies determine the companion properties. LMXBs allow us to study various physical mechanisms that define the current Galactic population such as the common-envelope formation efficiency, gravitational wave emission, magnetic field evolution and strength in old NSs and the age of a stellar population in general.

The accretion disk mediates the accretion flow onto the NS/BH analogous to CVs (Section 1.1.2). van Paradijs and McClintock (1994) found that the absolute visual magnitudes of 18 LMXBs are between $\sim 5$ and $\sim -5$, with such a large range attributed to the range of X-ray luminosities and accretion disk size. This indicates it is the reprocessing of X-rays through the disk that dominates the optical spectrum in outburst although it has been suggested an irradiated face of the companion could contribute to the optical (however this face may be shielded for large portions of the orbital cycle). Moreover, in a toy model assuming an isotropically-emitting blackbody disk (van Paradijs and McClintock, 1994) show that $L_V \propto L_X^{1/2} P^{2/3}$ where the dependence on orbital period reflects that smaller disks have higher average temperatures, and the blackbody distribution shifts a larger fraction of its flux into the UV at the expense of optical emission. In quiescence, the disk is cool and the optical spectrum is dominated by the donor ($V \sim 16 - 23$, Lewin and van der Klis, 2006), which can allow the measurement of $f(M)$ using spectral type, period and $K_2$. The optical spectra of LMXBs show blue continua with broad, superimposed H and He emission lines that reflect the velocity dispersions in the inner disk

region. For persistent sources with NS primaries, there exists a tight correlation between absolute near-IR magnitude and orbital period (Revnivtsev et al., 2012) analogous to van Paradijs and McClintock (1994) for the optical V, with the assumption that the NIR could have a non-zero synchrotron contribution from a jet (Shahbaz et al., 2008).

Almost all Galactic BHs and many NSs are found in XRBs and the current sample of Galactic XRBs is dominated by bright ($L_X > 10^{36}$ erg/s) transient systems making it under-filled by those in long periods of quiescence. Quiescent LMXBs and CVs both have X-ray luminosities of $\sim 10^{30.5} - 10^{32.5}$ erg/s and are best identified with deep X-ray data and precise positional resolution (Grindlay et al., 2005), although distinguishing the two generally requires a direct mass measurement of the compact object. The deeper potential well of a NS or BH creates a larger $L_X$ for a given $\dot{M}$ and so $F_X/F_{opt}$ is a useful discriminant; CVs are not thought to exceed $L_X \sim 10^{34}$ erg/s. Particularly quiet/distant systems produce low numbers of X-ray counts making statistical inference difficult.

## 1.2 The Galactic Bulge Survey (GBS)

In Chapter 2 we present our recent work with the Galactic Bulge Survey (GBS), a wide and shallow *Chandra* X-ray survey of 12 square degrees above and below the Galactic Plane (Jonker et al., 2011). The purpose of this survey was to homogenize the Galactic X-ray sample by uncovering $> 100$ new quiescent LMXBS to ultimately put constraints on the common-envelope evolution in XRBs and the mass distribution of BHs and NSs. The survey depth was chosen to optimize LMXB detections over foreground CVs and the survey is out of the plane enough to allow optical and IR follow-up. Spectral observations are crucial in deriving compact object masses - the $H\alpha$ shape and width can be used to identify the presence of an accretion disk or a BH-primary (Casares, 2015, 2016) and the aforementioned Bowen fluorescence transitions at $4640 - 4650$Å

can identify the companion. The GBS photometric and spectroscopic follow-up is on-going and many compact systems have already been identified; however, many X-ray sources have multiple optical or IR counterparts within the positional error circle of *Chandra*. Greiss et al. (2013) and Wevers et al. (2016a) performed a matching analysis for the GBS in deep IR and optical observations, respectively. A UV analysis has not yet been completed, although some *Swift* pointings in the GBS region have been analyzed for *Swift* UVOT (Fielder et al., in prep). The extinction in the GBS region is lower than directly in the Galactic Plane, but not as low as sightlines outside of the main Galactic mass entirely. Accordingly, since UV radiation is preferentially absorbed by the interstellar medium over other bands a UV analysis will retrieve physically close objects, those in windows of particularly low extinction and those that are inherently UV bright. In Chapter 2, we perform a UV counterpart analysis using *GALEX* data in the near-UV and use the statistical likelihood of an X-ray/UV match to constrain optical and IR observations allowing multi-wavelength analysis for 269 GBS systems.